The small-scale high-frequency ExB instability and its links to observed features of the Hall thruster discharge

IEPC-2013-261

Presented at the 33rd International Electric Propulsion Conference,
The George Washington University, Washington, D.C., USA
October 6–10, 2013

Sedina Tsikata*
ICARE, Electric Propulsion Team, UPR 3021 CNRS, Orléans, France

Cyrille Honoré† and Dominique Grésillon‡
LPP, Ecole Polytechnique, UMR 7648 CNRS, Palaiseau, France

Anne Héron§
CPHT, Ecole Polytechnique, UMR 7644 CNRS, Palaiseau, France

Nicolas Lemoine¶ and Jordan Cavalier‖
IJL, UMR 7198 CNRS, Nancy, France

Collective Thomson scattering has been used in recent years to provide experimental characterizations for the electron cyclotron instability believed to contribute to anomalous electron transport at the Hall thruster exit plane. A new phase of experiments is underway studying the link between the mode and its features to the observed global features of the discharge, such as the discharge current. The mode is shown to be present at high amplitudes in regimes of strong discharge current oscillation, and its amplitude is strongly influenced by the use of a zero-emissivity wall material. The mode amplitude is successfully damped via the injection of a light gas species into the anode.

Nomenclature

$\vec{E}$	= electric field
$\vec{B}$	= magnetic field
$\vec{k}$	= observation wave vector
$S(k,\omega), S(k)$	= dynamic form factor, static form factor
SEE	= secondary electron emission
$\vec{V}_d$	= azimuthal electron drift velocity
I_d	= discharge current
T_e	= electron temperature

*Research Physicist, Electric Propulsion Team, ICARE, sedina.tsikata@cnrs-orleans.fr
†Research Engineer, Laboratoire de Physique des Plasmas, cyrille.honore@polytechnique.edu
‡Professor Emeritus, Laboratoire de Physique des Plasmas, dominique.gresillon@polytechnique.edu
§Research Physicist, Centre de Physique Théorique, anne.heron@polytechnique.edu
¶Assistant Professor, Institut Jean Lamour, nicolas.lemoine@ijl.nancy-universite.fr
‖PhD student, Institut Jean Lamour, jordan.cavalier@ijl.nancy-universite.fr

I. Introduction

COLLECTIVE Thomson scattering has been used in recent years for the study of plasma instabilities at the Hall thruster exit plane. Due to the unsuitability of electrostatic probes for investigations of the plasma in this region of the plume, it has become necessary to call upon new diagnostics to investigate the role of plasma turbulence in increasing electron mobility. The PRAXIS diagnostic has permitted the identification of a MHz-frequency, mm-wavelength azimuthal instability shown in numerical simulations[1] to drive an electric current across the device.

Despite the low electron densities in the thruster plasma, in comparison to densities encountered in fusion-type plasmas where the technique is more commonly used, the specially-adapted diagnostic has permitted descriptions of the mode dispersion relation, directivity and angular extent[2,3]. An examination of the linear kinetic theory solutions to the mode dispersion relation in the context of experimental results has also been performed[4].

The possible transport mechanism for this instability may be one analogous to the stochastic heating mechanism for tokamaks proposed by Karney[5], and applied in the Hall thruster context by Ducrocq and colleagues[6]. The determination of the proportion of axial current which may be directly attributed to the cyclotron instability is clearly complicated by the number of phenomena at work whose individual contributions are unknown, such as wall emission. Nevertheless, an attempt has been made in recent studies to determine how the mode characteristics influence (and are influenced by) different thruster operating regimes. Some of these preliminary experiments are described in this paper.

II. An overview of the diagnostic

In this collective scattering application to thruster studies, the observation length scales of the diagnostic are set to those of the unstable mode wavelength. The technique is distinct from the more commonly-known incoherent Thomson scattering, in which length scales smaller than the electron Debye length are probed. In this application, length scales at which electron positions are correlated (as would be observed in the presence of a wave propagating in the plasma) are examined. This has been applied in order to identify the predicted instability.

The diagnostic used is known as PRAXIS, and is a high-performance collective scattering bench which allows the detection of electron density fluctuations in low-density plasmas. This is achieved through a combination of the choices. The optical elements and laser have been chosen to minimize losses and provide a large scattered signal. High resolution and very high sample depth acquisition are necessary to allow the reduction of the signal variance through averaging. The diagnostic uses a monomode, continuous CO_2 laser of 10.6 μm wavelength and 40 W power.

The diagnostic observation wave vector $\vec{k}$ is defined by the Bragg relation: $\vec{k} = \vec{k_s} - \vec{k_i}$, where $\vec{k_s}$ is the scattering wave vector and $\vec{k_i}$ the incident wave vector. Two beams are used to define the observation wave vector: a local oscillator, frequency-upshifted by 60 MHz with respect to the initial laser frequency and mixed with the plasma-scattered radiation, and a primary beam. The overlap of the two beams in the plasma forms the observation volume, which in this application crosses the entire thruster diameter, but is typically placed to favor observations of one channel.

The wave vector magnitude is modified using a translator-rotator element on the optical bench which changes the angle of intersection of the beams (on the order of a few mrad). The wave vector orientation is modified using this element, allowing two planes to be examined: the $(\vec{E} \times \vec{B}, \vec{E})$ plane and the $(\vec{E} \times \vec{B}, \vec{B})$ plane. The mixing of the reference local oscillator and the plasma-scattered radiation form part of a heterodyne detection scheme which allows the recovery of both phase and amplitude information of the scattered field. The modulated signal received on the detector is demodulated, filtered and amplified, and recorded on an acquisition card at 100 MHz. The discharge current of the thruster is simulataneously recorded on the acquisition card, as well as the detector continuous current, used to normalize the signal.

Four types of records are used, representing the various conditions used to determine the signal due purely to plasma scattering. These are the: plasma + local oscillator signal, plasma + local oscillator + primary beam signal, local oscillator + primary beam signal and the signal with the detector closed. The normalization procedure removes noise contributions and the normalized spectra provide a measure of the density fluctuation over the spectral frequency range, $S(k, \omega)$. The dynamic form factor signal, integrated over the frequency range in which the signal appears, gives the unitless "static form factor", $S(k)$, used in

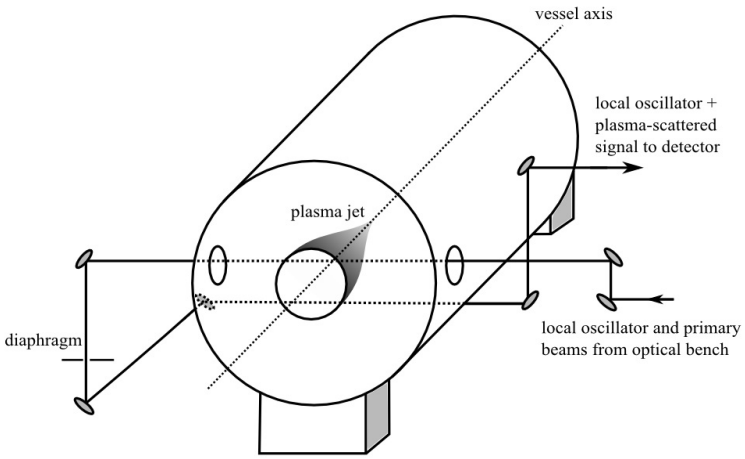

Figure 1. Simplified view of beam trajectories across the thruster plasma and redirection for recovery on the optical bench

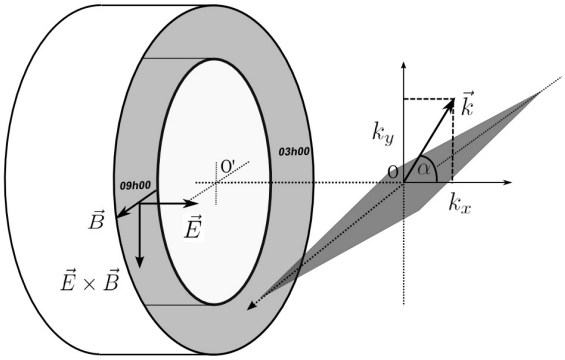

Figure 2. Thruster coordinate system and scattering volume (dark gray), defined by the local oscillator and primary beam intersection

subsequent discussions to describe the density fluctuation intensity. The mode frequency associated with a particular wave number is the mean frequency obtained from a Gaussian fit to the dynamic form factor signal.

Additional details concerning technical aspects of the original diagnostic and the signal normalization procedure may be found elsewhere[7]. Fig. 1 shows the direction of the local oscillator and primary beams across the vacuum vessel windows and thruster volume, and the recovery of the plasma-scattered radiation and local oscillator on the bench detector using a series of mirrors. Fig. 2 shows the thruster coordinate system: $\vec{E}$ is aligned with the thruster axis, and $\vec{B}$ with the radial direction. The angle α is changed on the bench; α is zero along the E-field direction and increases in the anticlockwise direction. Observations of the $\vec{E} \times \vec{B}$ mode in this paper occur around the α = -90° direction. The maximum signal amplitude in most situations is observed with $\vec{k}$ oriented at -100°, as described in a previous paper[3].

The direction of the azimuthal drift, $\vec{V_d}$, implies that positive frequency peak observations occur at the 09h00 channel (with channels viewed facing the thruster). The current diagnostic setup places the observation volume primarily for observations of this channel.

The experiments described in this paper concern two laboratory model thrusters: the 5 kW PPS®X000 thruster, and the 1.5 kW PPS®1350-ML thruster. Measurements are made with the observation volume at a distance of 11 mm from the exit plane unless otherwise indicated; this distance corresponds approximately to the location of the highest mode fluctuation amplitude in the axial direction.

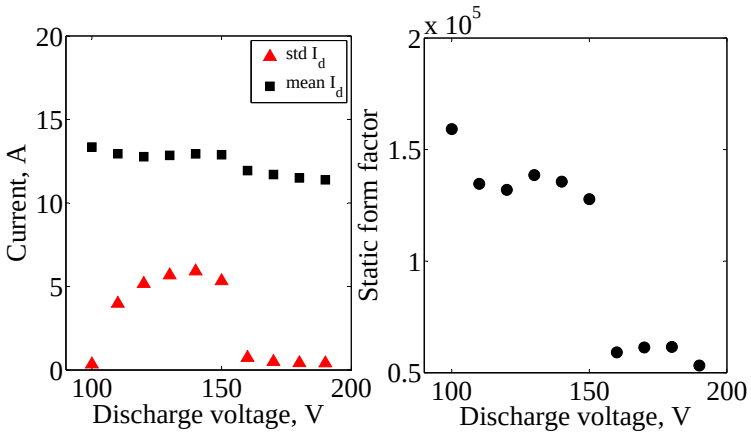

Figure 3. Fluctuations in discharge current mean and standard deviations (left) and azimuthal mode amplitude (right) at low discharge voltages

III. Regimes of high discharge current oscillation

A number of low-voltage regimes are examined for the PPS®X000 thruster, which has a nominal operating voltage of 500 V. The discharge current is generally stable for a wide range of operating voltages, however, at low voltages large amplitude jumps in the discharge current signal may be observed. The mode fluctuation amplitude at a fixed angle α of -100°, for voltages ranging from 100 to 190 V, is determined. The observation wavenumber is set at an arbitrary value of about 5300 rad/m, and the gas flow rate (xenon) to 12 mg/s. The magnetic field magnitude is 150 G in the center of the channel.

In Fig. 3, the overall mean discharge current is observed to drop slightly, by 2 A, as the voltage is increased from 100 to 190 V. However, the change in the standard deviation of the discharge current is more marked, with a variation by over a factor of ten between the maximum and minimum values. The important drop in the discharge current fluctuation amplitude at 150 V is reproduced in the azimuthal mode amplitude, as shown in Fig. 3.

An increase in the discharge voltage should increase the drift velocity at constant magnetic field. It is assumed here that the axial shift of the maximum amplitude of the electric field is minimal for the voltage range explored. All things being equal, an increase in $\vec{V_d}$ should be associated with an increase in the mode growth rate, and this should be reflected in the observed amplitude. However, the opposite is true here. It is also worth mentioning that the ionization efficiency of this thruster is expected to be lower at low voltages, and the electron density would be expected to be somewhat lower than in nominal regimes, which would reduce the mode amplitude to some degree. The higher mode amplitudes observed at low voltages thus appear to be a true reflection of a larger fluctuation amplitude which is not attributable merely to changes in the local plasma conditions.

At present, it is too early to establish whether these high-fluctuation regimes are due to the presence of the azimuthal mode at high amplitudes. The azimuthal mode, with a larger amplitude in such regimes, could play a role in maintaining the discharge by increasing the electron mobility. As will be discussed later on in this paper, the understanding of the role played by this mode in transport is complicated by additional effects which are revealed in radial-azimuthal numerical simulations.

IV. Control of mode amplitude

One question which has arisen is whether, given the role played by the mode in increasing the axial mobility, its amplitude can be modified directly. One way this is achieved is by the introduction of a small proportion of a lighter gas such as hydrogen into the main xenon anode supply. The wave measured experimentally is not strongly damped due to the slow response of heavy xenon ions, however, such damping

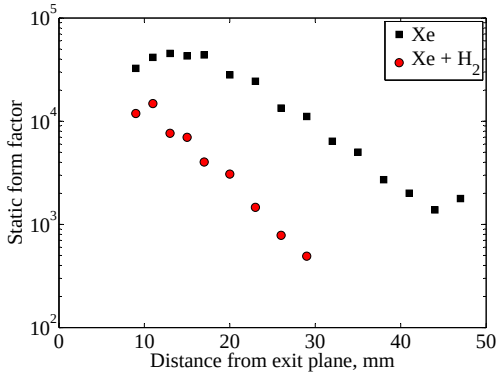

Figure 4. Attenuation of azimuthal mode amplitude with the addition of hydrogen ions

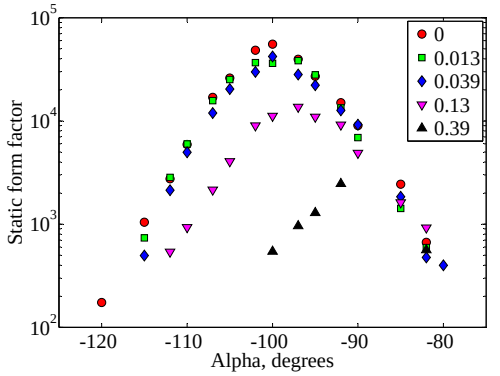

Figure 5. Attenuation of azimuthal mode amplitude and modification of mode directivity with the addition of hydrogen ions

could be increased through the creation of lighter ions within the plasma with a faster response.

A small percentage (13% by volume) of hydrogen is introduced into the anode supply. The variation in the mode amplitude with axial distance from the thruster is measured. The addition of hydrogen leads to a steeper exponential drop in the mode amplitude and an overall lower mode amplitude, as shown by Fig. 4.

The addition of different proportions of hydrogen reveals that both the mode directivity and amplitude are affected, as is clear from Fig. 5. For proportions higher than 0.039, the damping becomes noticeable and is accompanied by a shift in the location of the angle at which the maximum signal is observed. This shift corresponds to the mode propagating in a more azimuthal direction, as opposed to inclined towards the thruster face in the $(\vec{E} \times \vec{B}, \vec{E})$ plane under normal conditions. An examination of the discharge current reveals a slight increase with the proportion of hydrogen. However, careful measurements of the ionization degree of the added hydrogen and the ion current will be needed for further interpretation. The effect of increasing background pressure must also be taken into account at the highest hydrogen proportion. For now, the addition of hydrogen appears to be an effective method of damping the azimuthal fluctuations.

V. Wall material effect on mode fluctuation

Recent azimuthal-radial particle-in-cell simulations[10] show that the interplay between secondary electron emission and the electron cyclotron instability is extremely complex. The instability is shown to cause heating of the plasma in the azimuthal and radial directions, an effect which can increase the wall emission and change the sheath potential. The beam-plasma instability reported in other works[8,9] has been observed, associated with a jump in the conductivity due to SEE. The cooling of the plasma due to SEE would lower the azimuthal mode amplitude, but not damp it entirely.

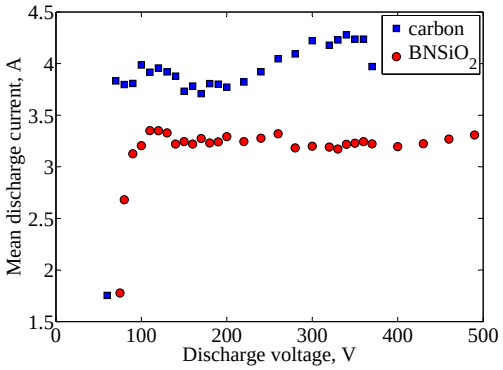

Figure 6. Variation in mean discharge current with applied voltage for carbon velvet and $BNSiO_2$ walls

The axial electron current as a function of time for materials of different electron emission energies has been determined in the azimuthal-radial simulations[10]. At the start of a simulation, the axial currents are identifical because they are attributable to the cyclotron instability alone, with the same values of drift velocity and electron temperature applied for all materials. Later on in the simulation, following a period of heating of the bulk plasma by the instability, the beam-plasma regime in which electron streams appear at the walls occurs, and a jump in the axial current is observed. A material with zero emission was shown to display no such transition in current.

As pointed out by the authors, the coupling (and coexistence) of SEE and the azimuthal instability means that the identification of the current due to the fluctuations or to SEE alone is likely to be impossible. However, we can attempt to examine how the azimuthal mode features and discharge behavior are modified by the use of a non-emitting material. This material consists of carbon fibers on a graphite substrate and is considered for this study due to its suppression of electron emission. The use of this material in experiments was first performed by Raitses and colleagues[11]. They provided measurements of electron temperature, electric field profiles and mobilities showing a drastic influence of the material on properties of the discharge.

The influence of the wall material on microturbulence at the thruster exit is the subject of this section. Experimental observations are made beyond the exit plane, whereas PIC simulations were performed at a fixed axial distance within the channel. However, as the density fluctuations measured by the diagnostic have been shown to be convected axially, it is possible that the material influence on the instability may still be detectable even some distance outside the channel.

These experiments concern the PPS®1350-ML, which has a nominal operating voltage of 300 V. Floating electrodes of carbon velvet replace the last 8 mm of the $BNSiO_2$ exterior and interior walls. This width is expected to sufficiently cover the acceleration zone within the channel where the azimuthal mode is believed to first develop. The xenon anode supply rate used is 3.5 mg/s, and the magnetic field magnitude is 150 G in the center of channel. Comparisons are made with channels consisting of $BNSiO_2$ alone.

An examination of the discharge current is made over a range of voltages. It is notable that the applied discharge voltage using carbon velvet can be reduced to be as low as 60 V before the discharge is extinguished, however, the discharge is difficult to sustain above 370 V and shuts off after a few minutes. In contrast, the lower limit on the applied voltage for $BNSiO_2$ is higher (75 V) and voltages beyond 450 V at this flow rate are applied, with the only limit being the 1.5 kW power rating of the thruster.

In the range of voltages explored, the discharge current remains relatively flat for borosil walls, a feature which is different from the linear increase expected (Fig. 6). The carbon velvet shows a slight increase in discharge current at higher voltages, and discharge currents are consistently higher than with borosil walls. Unfortunately, electric field measurements are not yet available from these tests. However, as shown by Raitses et. al., the use of carbon velvet electrodes allows the achievement of higher electric field amplitudes, and higher maximum T_e values. Though the wall conductivity has been reduced, other mechanisms such as plasma instabilities, dependent on the local electric field, may play a role in increasing the mean current value.

The discharge current standard deviation shows important differences between the two materials. Both materials show sharp peaks in the discharge current fluctation at low voltage (100 V for carbon, 110 V

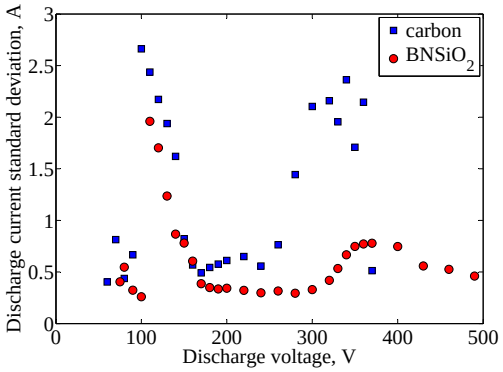

Figure 7. Discharge current standard deviation with applied voltage for carbon velvet and $BNSiO_2$ walls

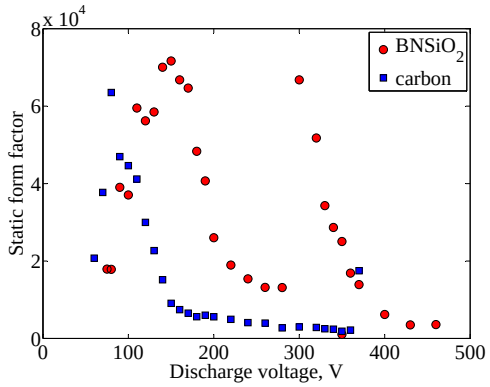

Figure 8. Variation in azimuthal mode fluctuation intensity with applied voltage for carbon velvet and $BNSiO_2$ walls

for borosil). The carbon velvet electrodes show two later peaks around 220 and 340 V. Borosil walls also show a second peak at higher voltages. Discharge current fluctuations are markedly larger for carbon velvet, particularly at the higher voltages.

These results can possibly be interpreted in the context of the variation of the azimuthal mode fluctuation intensity with voltage, shown in Fig. 8. For borosil walls, the large jumps in the discharge current fluctuation amplitude appear to coincide quite closely to the regimes of high azimuthal mode fluctuation. The fluctuation intensity is smaller with carbon velvet electrodes, which is unexpected. It likely that even though higher electric field amplitudes are achieved for the carbon velvet electrodes for the same applied voltage as for borosil, the location of the electric field peaks differ for the two materials[11]. For the maximum field located at the exit plane or further inside the channel for carbon electrodes, measurements made in the experiment 11 mm from the exit plane may already be in a location where the field amplitude has dropped significantly. The mode amplitude may have decreased from an initial peak further upstream. Upcoming experiments and measurements of the electric field should clarify these points.

VI. Conclusion

When different thruster operating regimes and wall materials are explored, the fluctuation amplitude of the electron cyclotron instability, and possibly its contribution to transport, are observed to differ. The mode amplitude is highest in regimes in which the discharge current shows large-amplitude oscillations. The fluctuation intensity is strongly affected by the use of non-emitting walls, possibly due to the altering of the electric field profile. The mode amplitude can be directly damped through the creation in the plume of a light ion species. Complementary measurements of thruster performance and using other diagnostics will be

valuable for completing interpretations of the mode behavior.

Acknowledgments

Funding for this work was provided by CNES. The authors thank the PIVOINE technical staff: G. Largeau, S. Sayamath, G. Daniel and P. Lasgorceix. S.T. thanks Dr. Y. Raitses and Dr. T. Knowles of Energy Science Laboratories, Inc., for information concerning the use of the carbon velvet electrodes.

References

[1]Adam, J.C, Héron, A., and Laval, G., "Study of stationary plasma thrusters using two-dimensional fully kinetic simulations," *Phys. Plasmas*, Vol. 11, No. 1, 295, 2004.

[2]Tsikata, S., Lemoine, N., Pisarev, V., and Grésillon, D., "Dispersion relations of electron density fluctuations in a Hall thruster plasma, observed by collective light scattering," *Phys. Plasmas*, Vol. 16, 033506, 2009.

[3]Tsikata, S., Honoré, C., Lemoine, N. and Grésillon, D.,"Three-dimensional structure of electron density fluctuations in the Hall thruster plasma: ExB mode," *Phys. Plasmas*, Vol. 17, 112110, 2010.

[4]Cavalier, J., Lemoine, N., Bonhomme, G., Tsikata, S., Honoré, C. and Grésillon, D., "Hall thruster plasma fluctuations identified as the ExB electron drift instability: modeling and fitting on experimental data," *Phys. Plasmas*, Vol. 20, 082107, 2013.

[5]Karney, C. F. F., "Stochastic ion heating by a lower hybrid wave," *Phys. Fluids*, Vol. 21, No. 9, pp. 1584-1599, 1978.

[6]Ducrocq, A., Adam, J-C., Héron, A., and Laval, G., "High-frequency electron drift instability in the cross-field configuration of Hall thrusters," *Phys. Plasmas*, Vol. 13, 102111, 2006.

[7]Tsikata, S., "Small-scale electron density fluctuations in the Hall thruster, investigated by collective light scattering," Ph.D. Dissertation, Ecole Polytechnique, 2009.

[8]D. Sydorenko, A. Smolyakov, I. Kaganovich, and Y. Raitses, "Kinetic simulation of secondary electron emission effects in Hall thrusters, *Phys. Plasmas*, Vol. 13, No. 1, 014501, 2006.

[9]I. Kaganovich, Y. Raitses, D. Sydorenko, and A. Smolyakov, "Kinetic effects in a Hall thruster discharge," *Phys. Plasmas*, Vol. 14, No. 5, 057104, 2007.

[10]Héron, A. and Adam, J-C., "Anomalous conductivity in Hall thrusters: effects of the non-linear coupling of the electron-cyclotron drift instability with secondary electron emission of the walls," *Phys. Plasmas*, Vol. 20, 082313, 2013.

[11]Raitses, Y., Kaganovich, I. D., Khrabrov, A., Sydorenko, D., Fisch, N. J., and Smolyakov, A., "Effect of secondary electron emission on electron cross-field current in E x B discharges," .IEEE Trans. Plasma Sci., Vol. 39, No. 4, 995, 2011